Effects of relative humidity and CO(g) on the O_3-initiated oxidation reaction of Hg^0(g): kinetic & product studies

Graydon Snider , Farhad Raofie and Parisa A. Ariya

Abstract

Ozone is assumed to be the predominant tropospheric oxidant of gaseous elemental mercury (Hg^0(g)), defining mercury global atmospheric lifetime. In this study we have examined the effects of two atmospherically relevant polar compounds, H_2O(g) and CO(g), on the absolute rate coefficient of the O_3-initiated oxidation of Hg^0(g), at 296 ± 2 K using gas chromatography coupled to mass spectrometry (GC-MS). In CO-added experiments, we observed a significant increase in the reaction rate that could be explained by pure gas-phase chemistry. In contrast, we found the apparent rate constant, k_{net}, varied with the surface-to-volume ratio (0.6 to 5.5 L flasks) in water-added experiments. We have observed small increases in k_{net} for nonzero relative humidity, RH < 100%, but substantial increase at RH ≥ 100%. Product studies were performed using mass spectrometry and high resolution transmission electron microscopy coupled to an electron dispersive spectrometer (HRTEM-EDS). Our results give evidence for enhanced chain growth of HgO(s) on a carbon grid at RH = 50%. A water/surface/ozone independent ozone oxidation rate is estimated to be (6.2 ± (1.1; $t\sigma\sqrt{n}$) × 10^{-19} cm^3 $molecule^{-1}$ s^{-1}. The total uncertainty associated with the ensemble of experiments amount to approximately ≤20%. The atmospheric implications of our results and the effect of an added reaction partner in homogeneous and heterogeneous atmospheric chemistry will be discussed.

Introduction

Elemental mercury is a very toxic heavy metal in the Earth's ecosystem. Estimates of the tropospheric lifetime of gaseous elemental mercury, Hg^0(g), range between 0.7–1.7 years[1–5] with a ~98%[6–8] abundance relative to particulate (Hg_p) and oxidized (Hg(II)) mercury. Recent studies in the marine boundary layer and in the polar-regions indicate that mercury lifetimes can be much shorter, potentially due to the presence of reactive halogen oxidants.[9] Background concentrations in the northern hemisphere have been measured at 1.3–1.7 ng m^{-3} (0.16–0.21 *parts per trillion*).[10]Mercury is eventually removed from the atmosphere through wet and dry deposition.[1,11]

In our previous laboratory studies we focused on the oxidation of elemental mercury by halogens, halogen oxides (XO; X = Cl, Br, I), $OH^{\cdot}$, and ozone.[12–15] In those experiments we varied temperature, photochemical sources, different surfaces, chemical probes, scavengers, and reactant concentrations to obtain several mercury oxidation rate constants. Among these oxidants considered, ozone was regarded as the among the most important mercury-depleting compounds in the troposphere outside marine or polar regions.[1]

Previous studies have shown that the apparent rate constant for the oxidation of Hg^0(g) can be increased if water is present; Menke and Wallis[16] found the rate of mercury oxidation by chlorine will triple when increasing RH to 80%. A later study by Lindqvist and Iverfeldt[17] observed that the

presence of liquid water and ozone together will enhance deposition of $Hg^0(g)$. The mechanism of this water catalysis, whether through aerosols or the gas-phase, remains imprecise.

We have previously studied ozone-addition with elemental mercury under dry conditions.[13] The net reaction is written:

$$Hg^0(g) + O_3(g) \xrightarrow{k_{net}} HgO(s) + O_2(g) \qquad (1)$$

Calvert and Lindberg[18] suggest reaction (1) could proceed by an addition of ozone, followed by a re-arrangement into the linear species OHgOO:

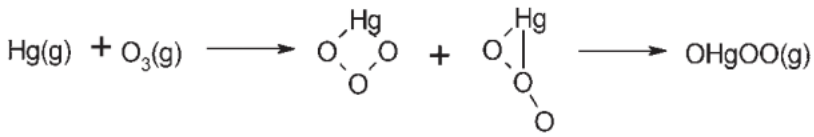

(2)

The reaction may be followed by dissociation into O_2 and HgO(g), the latter precipitating immediately to HgO(s).

$$OHgOO(g) \rightarrow HgO(g)\ (\rightarrow HgO(s)) + O_2(g) \qquad (3)$$

The dissociation and precipitation are essentially irreversible steps.

The apparent rate constant, k_{net}, reaction (1), was previously found by our group[13] to be $(7.5 \pm 0.9) \times 10^{-19}$ cm^3 molecule^{-1} s^{-1}, in good agreement with Sumner *et al.*:[19] $(6.4 \pm 2.3) \times 10^{-19}$ cm^3 molecule^{-1} s^{-1} (performed in a much larger 17 m^3 chamber where heterogeneous reactions were significantly reduced by a decrease in the surface-to-volume ratio). Our rate constant was found to be larger than an earlier study by Hall[20] $(0.3 \pm 0.2) \times 10^{-19}$ cm^3 molecule^{-1} s^{-1}, and smaller than both Schroeder's[7] value, 49×10^{-19} cm^3 molecule^{-1} s^{-1} (no error reported), and Iverfeldt's[17] value, 20×10^{-19} cm^3 molecule^{-1} s^{-1} (no error reported).

Our present experiment evaluates the effect of the third bodies, H_2O and CO, on the apparent rate coefficient, k_{net}. The elementary reaction of interest is the reversible association of $Hg^0(g)$ and O_3:

$$Hg^0(g) + O_3(g) \leftrightarrow HgO_3(g) \qquad (4)$$

where the intermediate HgO_3 is expected to decompose spontaneously and irreversibly into HgO(s).

$$HgO_3(g) \rightarrow \text{Products} \qquad (5)$$

We quantify the dependence of k_{net} on $H_2O(g)$, O_3, CO, and trimethyl benzene (TMB), surface-to-volume ratios, and to the presence of a polymer wax coating. A product study is presented for reactions in both humid and dry conditions, and the best estimate for dry $O_3(g) + Hg^0(g)$ reaction rate is provided. Some discussion on the implications for atmospheric mercury is presented.

Methods

Kinetic studies

The apparent rate constant of the $O_3(g) + Hg^0(g)$ reaction was determined by measuring the relative loss of $[Hg^0(g)]$ *via* electron impact (EI) ionization mass spectrometry (HP-5973). The experiments were performed under near-atmospheric conditions (750–770 Torr, $T = 296 \pm 2$ K) in

ultra high purity N_2. Experiments were carried out in 0.59, 1.1, 2.2, 3.1, and 5.5 l spherical Pyrex flasks supplied with a magnetic stirrer to stimulate mixing. The reaction flask was coated with MTO-Halocarbon Wax (Supelco) as an attempt to reduce surface adsorption of reactants, products, or reaction intermediates to lead undesired side and secondary reactions. Between runs, flasks were washed with concentrated nitric acid, scrubbed with a nylon brush with soap and water, washed with 18.2 MΩ milli-Q water, and then with HPLC-grade acetone. Halocarbon wax was reapplied through a 10% solution (by weight) of HPLC-grade acetone and dried at 120 °C for >1 hour. Samples from then N_2-filled reaction chambers (without reactants) were taken and analyzed using GC-MS to preclude the existence of detectable residual impurities. To prepare reaction mixtures, the reaction chamber was evacuated to a pressure of *ca.* 5×10^{-2} Torr with a two-stage pump (Savant VP 190) and flushed with N_2 gas 3–5 times. Mercury vapour in equilibrium with liquid mercury (under UHP N_2) was transferred *via* vacuum line to an evacuated wax-coated reaction flask, and filled to atmospheric pressure with nitrogen gas. The final concentration of mercury vapour in the reaction flask is calculated to be 1–2 ppm (1 ppm ~2.46×10^{13} molecule cm^{-3} at 298 K and 1 atm). To add humidity in all flasks, milli-Q water (Millipore, 18.2 MΩ) was introduced *via* a liquid-tight 10 μL syringe (Hamilton series 1700) to the flask. As ozone and trace hydrocarbons may react to form radical by-products, the scavenger 1,3,5-trimethyl benzene (TMB) was included.[21] TMB was injected as a liquid (Hamilton series 700) and allowed to vaporize in the chamber for >30 minutes. Ozone was produced using an ozone generator (model OL 100/DS, Ozone Services Inc.); the resulting O_3 mixture was then trapped in a *U*-shaped tube containing silica gel cooled to 195 K in a dry ice–acetone bath, and then transferred ozone to an evacuated flask. The ozone flask was brought to atmospheric pressure *via* UHP nitrogen. A UV-visible spectrophotometer (Varian Cary-50 Bio) determined the concentration of ozone to be injected. Decay of ozone is negligible within the time-frame of the experiment (<1% per hour). From Beer's law, $A_{\log 10} = \varepsilon[O_3]l$ (where ε_λ = 296.7 nm = (2.64 ± 0.05) × 10^{-19} cm^2 $molecule^{-1}$,[22] l = 10.28 ± 0.05 cm), specific amounts of ozone were transferred to the reaction flask using a gas-tight syringe with relative uncertainties of 2% (1σ). A Teflon-coated hygrometer probe (MC-P, Panametrics) indicated RH < 0.1% for 'water-free' runs, and measured within ±2% of expected values for RH = 10 to 90%. CO was obtained from a 99.99% pure gas source, filled into an evacuated flask, where the desired aliquots were taken.

We performed the separation of Hg^0(g) from other constituents on a gas chromatograph (HP-6890) equipped with a 30 m × 0.25 mm i.d. × 1.0 μm crossed-linked phenyl–methyl–siloxane column (HP5-MS). The column was operated at a constant flow (1.5 mL min^{-1}) of helium. During chromatographic runs, we typically kept the GC oven isothermal at 40 °C for 1 min and increased the temperature at a rate of 25 °C min^{-1} from 40 to 80 °C.

Arbitrary concentrations units of Hg^+(g) ions at m/z = 198–202 were monitored *via*single ion monitoring (SIM) through integrated peak areas. The observed isotopic ratios corresponded with the expected ratios 33 : 56 : 78 : 44 : 100. From our GC temperature program, the measured retention time of the mercury peak was at *ca.*, 1.3 min. The detection limit of Hg^0(g) was 10 ppb. Initial mixing ratios of the reactants were 1–2 ppm Hg^0(g), 10 to 60 ppm O_3, 0.0–31 parts per thousand H_2O (RH = 0–100%), 0.80 to 6.4 parts per thousand CO, and 90 ppm TMB. The volume of the injected gas sample was 200 μL *via* an 1825 Hamilton gas-tight syringe. TMB was deployed as a radical scavenger to capture undesired radicals, which could form from secondary reactions of ozone with impurities or reaction products and intermediates.[13]

The reaction of Hg^0(g) with ozone was assumed to behave under pseudo first-order conditions with respect to Hg^0(g) at T = 296 ± 1 K. To obtain the rate coefficient k_{net} for reaction (6), the ozone

concentration was assumed to remain constant. The method also assumes that ozone only reacts with elemental mercury. Ozone has a slow thermal loss resulting in O atom production, which might be the cause of additional Hg loss.

The rate-limiting step in reaction (6) is assumed to be the association of $Hg^0(g)$ and O_3. Hence,

$$-\frac{d[Hg^0(g)]}{dt} = k_{net}[O_3][Hg^0(g)] \qquad (6)$$

Integration of (6) yields slope $k' = [O_3]k_{net}$ when plotting $\ln([Hg^0(g)]_0/[Hg^0(g)]_t)$ *versus* time. This approximation is valid only if secondary reactions (*e.g.* with OH or other impurities) are negligible and ozone is in sufficient excess. The latter condition was only approximate; $6 < [O_3]/[Hg^0(g)] < 40$; $[Hg^0(g)] = 1.5$ ppm. Experiments were performed indicating the addition of TMB and the halocarbon wax coating indeed improved linearity of slopes and appeared to affect the reaction rate (Fig. 1).

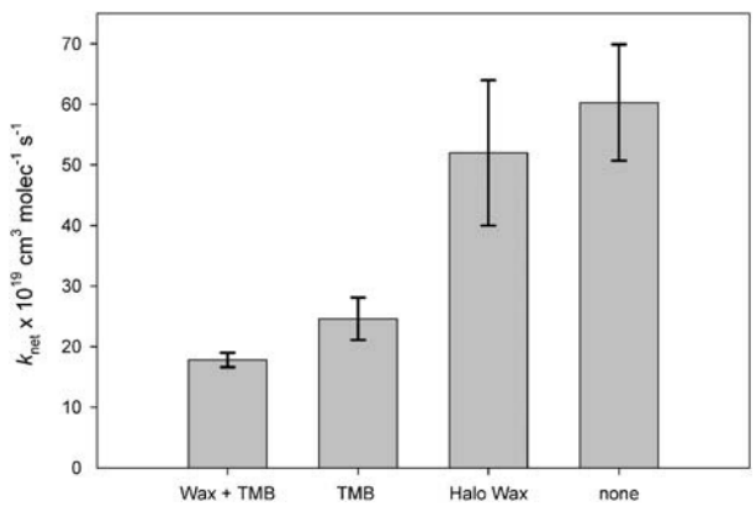

Fig. 1 Changes to the rate k_{net} *via* the addition of a halocarbon wax coating and/or the radical scavenger 1,3,5-trimethyl benzene (TMB). Conditions: 1L Pyrex flask, [TMB] = 90 ppm (0.5 μL), $[O_3]$ = 20 ppm. Note: increasing [TMB] to 360 ppm had a negligible effect on k_{net}. Errors are calculated to be $\pm t\sigma/\sqrt{n}$ (95% C.I.), where $n = 6$, and t is the t-test value for $n-1$ degrees of freedom.

Product study

Transmission electron microscopy . Reaction products were collected from the wall of the flask by placing carbon-coated Cu grids on the surface of the reaction flask and collecting the grids upon completion of the reaction. The elemental composition and the morphology of the collected products were analyzed using a high-resolution transmission electron microscope (HRTEM); model JEOL 2000. X-ray spectra were acquired with an electron beam size of 200 nm at 80 kV for 100 seconds (Fig. 2a and 3a) and HRTEM images from operating at 200 kV in bright-field mode at Scheerzer defocus conditions (Fig. 2b).

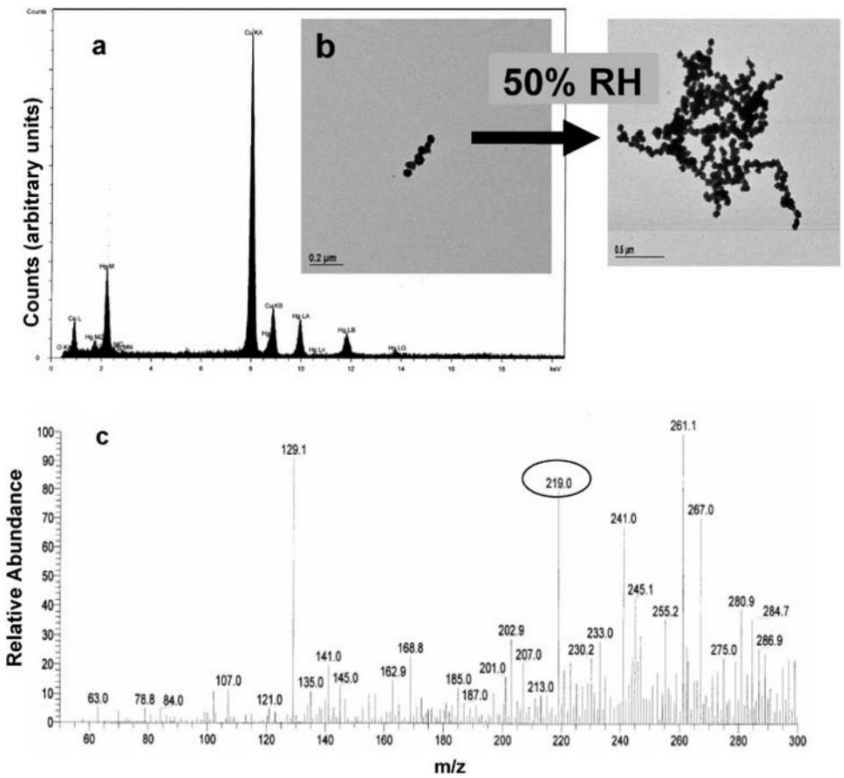

Fig. 2 (a) EDS image of HgO. (b) Comparative HRTEM image of HgO deposit at RH = 0% and 50%, and (c) CI of HgO product at RH = 0% and 50%.

Mass spectrometry studies. A gas sample of the reaction products were passed through a 1.1 mm i.d. × 10 cm length Pyrex tube (Corning) immersed in liquid nitrogen. The chemical structure of the reaction products mixture was identified using mass spectroscopy equipped with a chemical ionization (CI) source (Kratos MS25RFA). The probe temperature was elevated to 430 K. In the chemical ionization source, quasi-molecular ions $[M+H]^+$ are formed by proton transfer with NH_3 as the reagent gas.

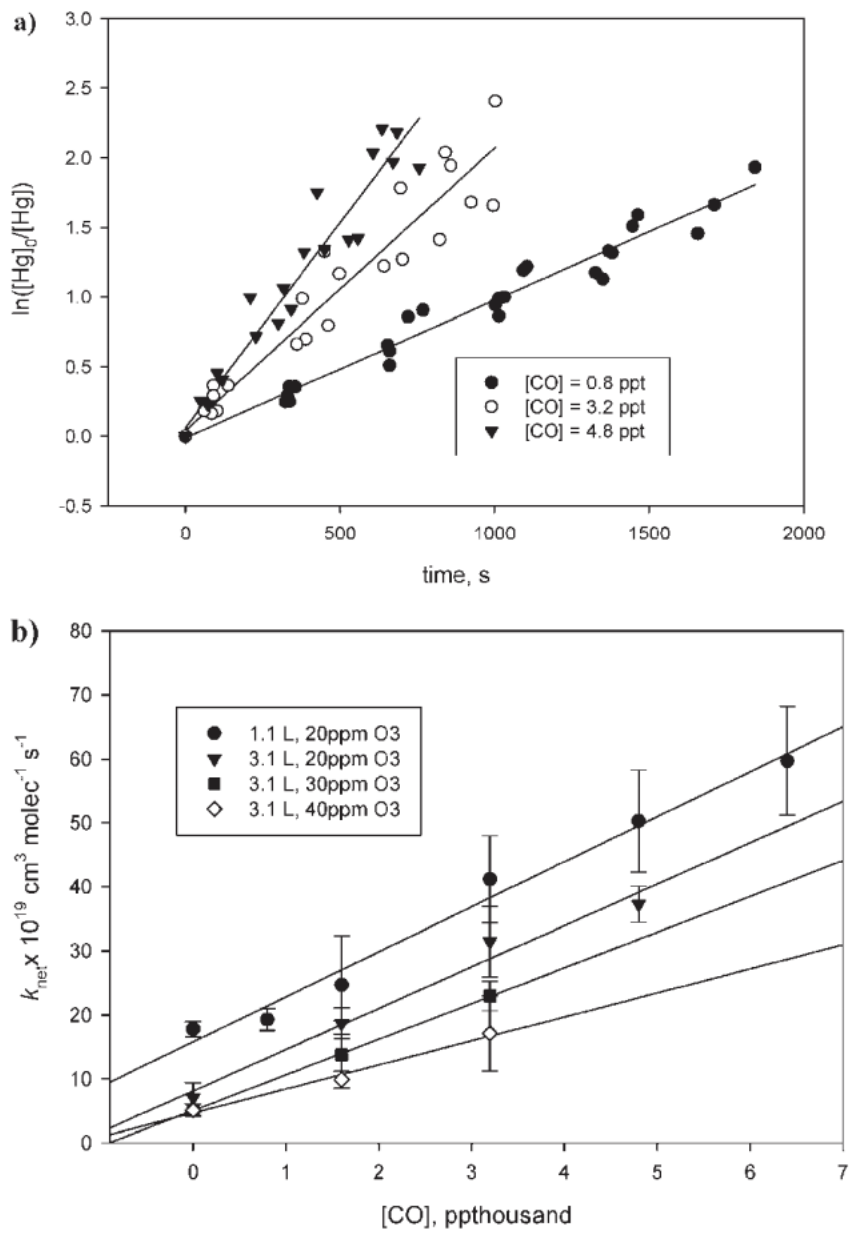

Fig. 3 (a) Typical pseudo first-order slopes of mercury decay using MS peak areas *versus* time (s) for three [CO] (pp *thousand*) values at 95% C.I. error. (b) Trend of an increasing rate constant with [CO] in a 1 L flask. Error bars report slope uncertainty at the 95% C.I.

Materials

Mercury (99.9995%) and trimethylbenzene (98%) were supplied by Aldrich. Carbon monoxide UHP (99.99%), Nitrogen UHP (5.0), and oxygen extra dry (2.6) were obtained from MEGS Gases Ltd. Mercury was further purified by transferred it to a gas-tight finger vial cooled at liquid N_2 temperature in a vacuum lines, and pumped for approximately 5 minutes at *ca.* 10^{-2} Torr.

Results and discussion

Kinetic results and potential mechanisms

The effect of CO. To further understand potential mechanism for third body dependence ozone oxidation of elemental mercury, we opted to use two polar gases, CO and water, as additional reactants. In Fig. 3b, the concentration of CO is approximately proportional to the rate k_{net}. Concentrations of CO were chosen to be $\sim 10^{17}$ molecules cm^{-3}; this concentration was also used in the water vapour experiments in the following section. Like water, CO(g) has a non-zero dipole moment.[23,24] It is known that CO may act as a radical scavenger,[25,26] though trimethylbenzene was our intended radical scavenger.[27] Given that CO concentrations were ~100 times greater than TMB, CO may have competed for reactive species. As 90 ppm of TMB appeared sufficient to scavenge reactive species, CO was not expected to significantly impact radical removal rates.

Slopes of ln([Hg^0(g)]) *versus time* were linear over a six fold range in CO concentration indicating the reaction was occurring under pseudo first order conditions (Fig. 3a). Data in Fig. 3b and Table 1 clearly show CO accelerates the oxidation of mercury. We performed two series of experiments (a) adding CO at the beginning of O_3 + Hg^0(g) reactions, and (b) adding after 20–40% mercury conversion by ozone. Our results of two experiments were similar, suggesting that the O_3–Hg^0(g) reaction was significantly accelerated using CO as the reactant. We did not see under experimental conditions a significant change in mercury concentration when we used only Hg^0(g) and CO(g) in the reaction chamber. We had initially considered the mechanism in the net reaction (1) to be gas-phase, unless CO was to adsorb on the halo wax-coated flask surface that may be unlikely, but it was not determined in this study. We did not observe any reactions under our experimental conditions between gaseous elemental mercury and CO. We hypothesize that CO associates with HgO_3 through reaction (4), which subsequently leads to product formation:

$$HgO_3 + CO \rightarrow \text{Products} \qquad (7)$$

The rate loss of mercury can then be written using elementary reactions (4–5 & 7) assuming steady-state concentrations of HgO_3:

$$-\frac{d[Hg^0(g)]}{dt} = k_4\left\{\frac{k_5 + k_6[CO]}{k_{-4} + k_5 + k_6[CO]}\right\}[Hg^0(g)][O_3] \qquad (8)$$

where the apparent rate is given to be

$$k_{net} = k_4\frac{k_5 + k_6[CO]}{k_{-4} + k_5 + k_6[CO]} \qquad (9)$$

Clearly k_{net} is hyperbolically dependent on [CO]. We interpret that much higher levels of CO cause a levelling off effect on k_{net}, but at lower concentrations k_{net} appears linear. It is noteworthy that the suggested above reaction schemes include only one way, and not exclusively, describing the observations in this study.

The effect of water vapour. We performed a series of experiments with $Hg^0(g)$ and water vapour alone (below saturation), and we did not observe any reactions under experimental conditions used in this study. Fig. 4 and Table 1 shows the effect of water (RH = 0 to 95%, $T \sim 296$ K) on the rate k_{net} in a 1.1 and 3.1 L flask. We have largely found the effect of water on k_{net} is negligible, consistent with Hall,[20] specifically for flasks ≥3 l. In a 1.1 L flask, the reaction rate increases slightly, between a factor of 1.1 and 1.7, though not with any obvious relationship to water concentration. We obtained a peak value of $k_{net} = (31.3 \pm 5.0) \times 10^{-19}$ cm^3 molecule^{-1} s^{-1} at 60% RH, however, due to the present magnitude of uncertainties we cannot suggest this to be a clear 'maximum'. Rates in a 1.1 l flask at RH = 20, 60, and 95% were repeated without the wax coating, and k_{net} increased by a factor of 1.2, 1.0 and 1.4, respectively, compared with the dry, untreated Pyrex flask rate constant. Flasks with untreated walls showed rate enhancement of 40–60% over halocarbon-coated flasks. At RH >100% (*i.e.* with a visible water mist coating inside the flasks), there is a significant change in the rate law; ln[$Hg^0(g)$] *versus* time is no longer linear. Acceleration of net reaction (1) due to condensed water has been previously noted by Iverfeldt and Lindqvist.[17] Our results show k_{net} is weakly (and nonlinearly) dependent on RH and that smaller S/V ratios (larger flasks) lessen statistically significant effects of water vapour. It is unknown the mechanistic details at this stage why $H_2O(g)$ does not exhibit similar behaviour to CO(g), however we hypothesize that water assisted reactions on surfaces may take place, whereas for CO, we have not seen under our experimental conditions any evidence for surface enhanced reactions.

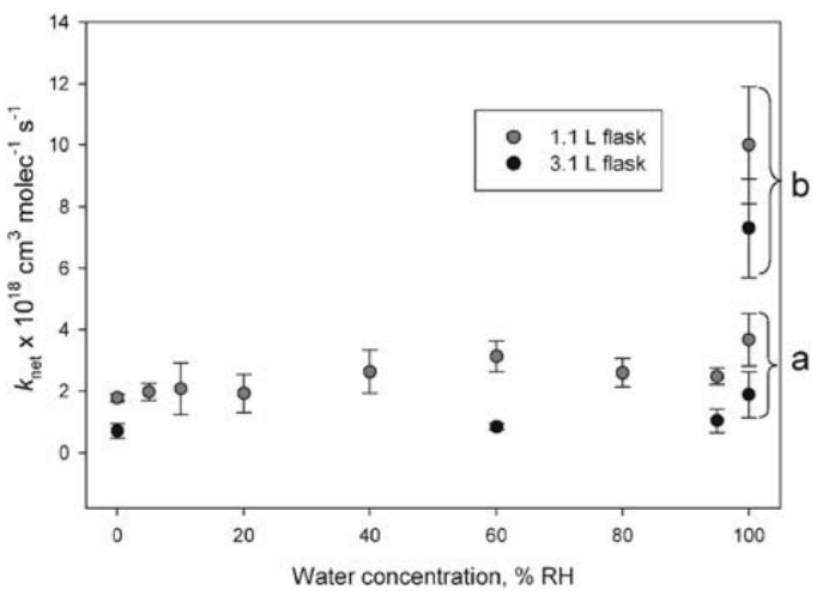

Fig. 4 Changes in rate constant, k_{net} ($295 \leq T \leq 298$ K), with respect to %RH in a 1.1 and 3.1 L flask. Errors of k_{net} are calculated at the 95% C.I. The uncertainty of RH is estimated at ±2%, omitted for clarity. At 100% RH, rates (a) are taken as the initial tangent to the slope k', and (b) is the rate at the latter half of the reaction.

Effect of TMB and wax coating. As shown in Fig. 1, the addition of TMB (~90 ppm) lowered the oxidation rate by a factor of three, as confirmed in previous studies.[13] Specifically, k_{net} decreases by $(35 \pm 11) \times 10^{-19}$ cm^3 molecule^{-1} s^{-1}. Mixtures of ozone and TMB alone did not produce a

significant decay for either species, nor was decay observed for $Hg^0(g)$ and TMB combined without ozone. Increasing TMB concentrations from 90 to 360 ppm did not lower rates further. The addition of the halocarbon wax coating reduced the oxidation rate by (7.4 ± 9.6) × 10^{-19} cm^3 $molecule^{-1}$ s^{-1}, which is not statistically significant. Combining halocarbon wax and TMB together lowered the rate to 30% of the original value. Although we have made steps to reduce heterogeneous reactions, we show that within the constraints of this experimental they are also unavoidable.

The effect of ozone. Fig. 5 depicts a decrease in our calculated k_{net} value with variable excess ozone concentrations (linearity is observed for individual $\ln[Hg^0(g)]$ *versus* time plots, *i.e.* $R^2 > 0.998$). This trend is similar to the $Cl_2 + Hg^0(g)$ data of Menke and Wallis.[16] In the previous study of reaction 1 by Hall,[20] there was evidence for heterogeneous ozone chemistry. Hall found the rate of $Hg^0(g)$ loss was equal to $k_{net}[Hg^0(g)][O_3]^{\beta}$, where $\beta = 0.81$. Our own analysis did not reveal a consistent β value for different flask volumes, ranging between 0.5 (1.1 l flask) and 1.4 (5.5 l flask).

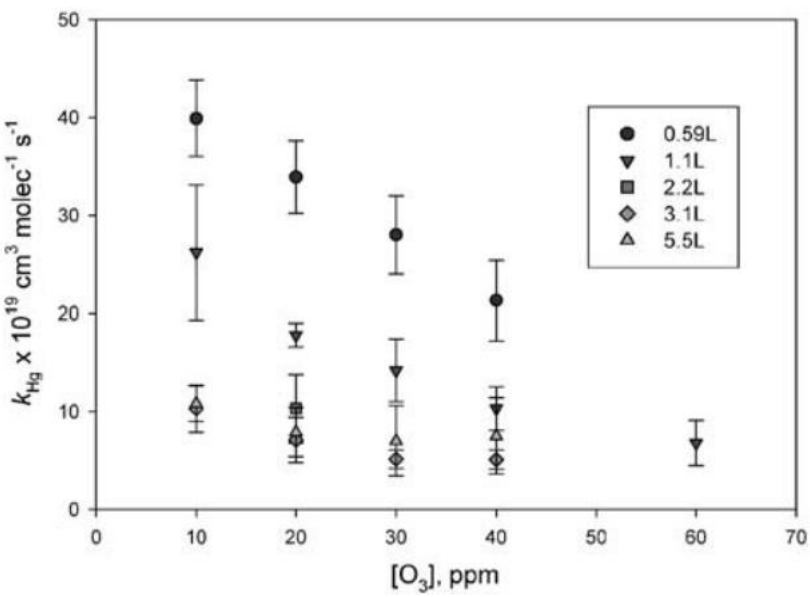

Fig. 5 Changes observed in the rate constant k_{net} due to various ozone concentrations and flask volumes. Error bars reported at the 95% C.I. The initial concentration of gaseous mercury, $[Hg^0(g)]_0$, is approximately 2 ppm.

Effects of surface. We expected the rate to increase with larger surface-to-volume (S/V) ratios (using 5.5, 3.1, 2.2. 1.1, and 0.6 l Pyrex flasks), shown in Fig. 5. The rate constants for 5.5 and 3.1 l flasks are statistically indistinguishable within 95% confidence level. This provides an indication that we have reached a limit to the S/V effect when halocarbon wax wall deactivation is performed. Larger flasks are also less affected by the changes in $[O_3]$, indicating some ozone is adsorbed to the flask walls with low surface-to-volume ratio (*i.e.*, 0.6 to 2.2 l flasks).

Empirically we observe k_{net} is proportional to S/V^2, or $1/r^4$, where r is the radius of the spherical flask. If we assume the rate of total mercury loss can be divided into two pathways: (i) by spontaneous oxidation within the volume of the flask, proportional to $V \cdot k_{vol}$, and (ii) by oxidation on the flask surface, proportional to $S/V \cdot k_{sur}$. Hence the total rate loss is

$$-\frac{\mathrm{dHg}}{\mathrm{d}t} = \left(Vk_{\mathrm{vol}} + \frac{S}{V}k_{\mathrm{sur}}\right)[\mathrm{Hg}][\mathrm{O_3}] \qquad (10)$$

Dividing eqn (10) through by flask volume V,

$$-\frac{\mathrm{d[Hg]}}{\mathrm{d}t} = \left(k_{\mathrm{vol}} + \frac{S}{V^2}k_{\mathrm{sur}}\right)[\mathrm{Hg}][\mathrm{O_3}] = k_{\mathrm{net}}[\mathrm{Hg}][\mathrm{O_3}] \qquad (11)$$

where $k_{net} = (k_{vol} + k_{sur} \times S/V^2)$. The apparent rate constant k_{net} is fixed for a given flask volume and ozone concentration (Fig. 6). By linear regression, we obtain $k_{vol} = (5.40 \pm 0.56) \times 10^{-19}$ cm^3 molecule^{-1} s^{-1} and $k_{sur} = (2.91 \pm 0.12) \times 10^{-15}$ cm^7 molecule^{-1} s^{-1} with linearity $R^2 = 0.995$. The surface rate loss k_{sur} has been previously discussed in the literature.[28] We note $Vk_{vol} = k_{sur}S/V$ when $V \sim 2.1$ L, hence surface reactions dominate $V < 2.1$ L.

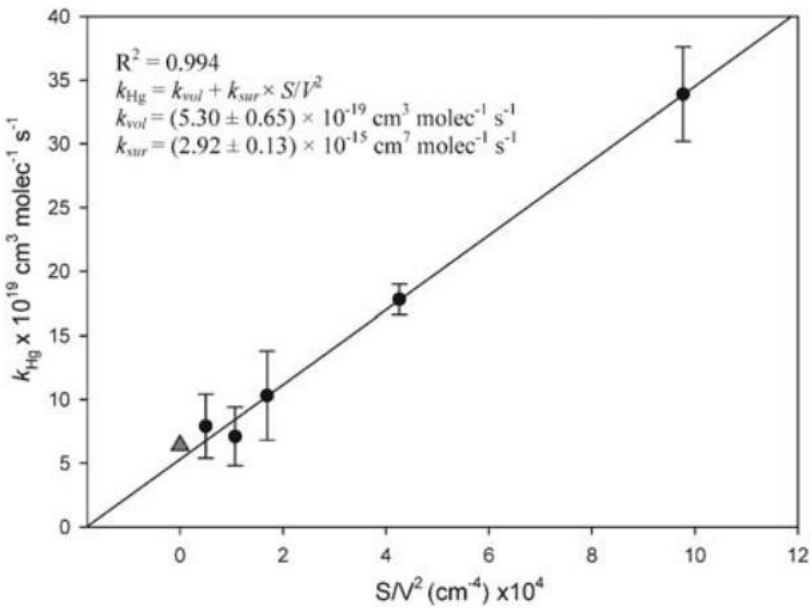

Fig. 6 Observed trend in the rate constant k_{net} due to changes in flask volume, and at constant ozone concentration; $[O_3]$ = 20 ppm. Left-most point (red) from Sumner *et al.*[19] Equation of best fit superimposed on graph. Error bars reported at 95% C.I.

Estimating k_{net} in reaction (1)

We compare two methods for obtaining a best estimate k_{net}. The first method uses the k_{net} values for $[O_3]$ = 30, 40 ppm in 3.1 and 5.5 L flasks (see the four points clustered together in Fig. 5). These k_{net} values are chosen due to their pseudo-first order behaviour, negligible sensitivity to ozone concentration change, and minimal S/V sensitivity. The slope average of the combined 24 (4 × 6) runs chosen in Fig. 5 leads to $k_{net} = (6.2 \pm 1.1) \times 10^{-19}$ cm^3 molecule^{-1} s^{-1} at a 95% confidence interval. In the second method we extrapolate the y-axis intercept in Fig. 6 ($S/V^2 \rightarrow 0$) obtaining $k_{net} = (5.8 \pm 3.4) \times 10^{-19}$ cm^3 molecule^{-1} s^{-1}. We judge that the first method provides the "best estimate" rate for reaction 1. In method 2 we cannot yet provide a sound mechanistic rationale. Hence, the value of $(6.2 \pm 1.1) \times 10^{-19}$ cm^3 molecule^{-1} s^{-1} represents the most reliable

value for an ozone-initiated oxidation of elemental mercury. Note that the total uncertainty associated with the ensemble of experiments amount to approximately ≤20%.

Product studies on reactions of O_3 + Hg^0(g) at RH = 0 and 50%

Since we observed potential evidence for heterogeneous reactions only in the presence of water vapour in contrast to CO, we performed additional product studies to further comprehend the nature of the products in water rich environment. In the EDS image (Fig. 2a), signals for Cu, Ca, Cl, and O are due to carbon-coated Cu grids. Solid HgO exists as a polymerized chain of Hg–O–Hg linkages.[29] The electron dispersive spectrum between RH = 0 and 50% is indistinguishable. We see in Fig. 2b that water vapour appears to encourage polymerization of HgO clusters, as clusters similar in size to 50% RH were not observed at 0% RH. As previously reported, 90% of HgO(s) is deposited on the flask walls under dry conditions.[13] The oligomerized form of HgO has very low vapour pressures[30] while extremely stable compared with the monomer.[31]

An EDS spectrum of the chemical composition of products in the gas–aerosol mixture revealed the gas–aerosol mixture contains mercury and oxygen. Due to the chemical composition of the reaction products, we expect aerosol should contain HgO(s), confirmed by MS analysis (Fig. 2c). Fig. 2c shows a signal at m/z = 219 for $HgOH^+$ (NH_3 was used as the reagent gas), the dominant mercury isotope ^{202}Hg. The m/z distribution also appears identical between 0% and 50% RH, and suggests humidity has little effect on the reaction products.

Exposure of the HgO(s) product (at RH = 50%) to $300 \leq \lambda \leq 400$ nm UV light for ∼10 min irradiation did not result in an appreciable change of product morphology determined by HRTEM imaging, nor elemental composition obtained *via*EDS.

Mechanisms for the formation of HgO(s)

It is clear reaction (1) is spontaneous based on the rapid loss of mercury through the introduction of ozone (precipitated as HgO(s)). A high-level *ab initio* study on the expected intermediate HgO(g), however, was performed by Shepler and Peterson,[32] who calculated a relatively weak dissociation energy: D_0 = 4.3 kcal mol^{-1}. A re-arrangement of mercury and ozone into HgO(g) + O_2(g) is calculated by Tossell to be endothermic, ΔE = +18 kcal mol^{-1}.[31] Reaction (1) is exothermic. Following the reaction coordinate between some transition intermediate Hg·O_3 and HgO(s), we expect a significant activation energy in forming HgO(g), followed by its exothermic precipitation. We hypothesize carbon monoxide will act as a catalyst to decrease the formation barrier energy of HgO(g) (see Fig. 7). Calculations for barrier energies of such a CO + HgO_3 complex may be the basis for further study.

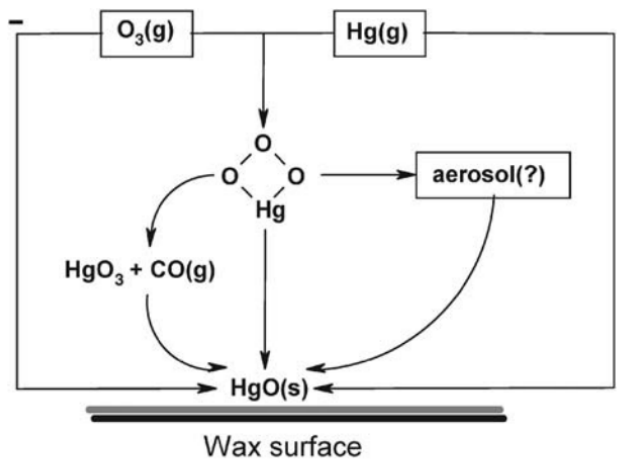

Fig. 7 Illustration depicting proposed gas-phase and surface reactions beginning with elemental mercury and ozone. Carbon monoxide here plays a side role in assisting the oxidation of the intermediate $Hg{\cdot}O_3$.

As noted by Sumner *et al.*,[33] microscopic layers of water may deposit onto a hydrophobic wax surface below 100% RH. In our study, the maximum rate constant afforded by the presence of water is $k_{net} = (31 \pm 4) \times 10^{-19}$ cm^3 molecule^{-1} s^{-1} (Fig. 4), far below the oxidation rate found in an aqueous environment, where $k = (800\,000 \pm 400\,000) \times 10^{-19}$ cm^3 molecule^{-1} s^{-1}.[34] Once water has condensed, the rate is seen to rapidly accelerate. Likely there are small increases in k_{net} through the presence of a thin water film. Fig. 6b provides our only evidence that HgO(s) growth and humidity are related. We must also consider the fact that these images were obtained over a carbon grid, and not the flask surface. We performed an additional sets of experiments in which HgO(s, yellow) powder were coated over a specific area (*ca.* 1/8 of surface) of the reaction chambers to evaluate the potential importance of HgO effect on the reaction rate enhancement. We noted an increase in the rate of Hg^0(g) removal similar in magnitude to the addition of liquid water. Exploration into the mechanistic understanding of water vapour's effect on the oxidation process is a desired future target.

Revised atmospheric lifetime of Hg^0(g) using the revised apparent rate constant

We have performed kinetic studies of Hg^0(g) oxidation by ozone over variable %RH, [CO], flask size, and $[O_3]_0$. Though product studies show HgO(s) will cluster more readily in the presence of H_2O, the Hg : O ratio, however, remains unchanged. Our kinetics show the rate constant k_{net} is marginally affected by increases in relative humidity below 100%, but proportional to CO concentrations in low parts per thousand. Our measurements of the apparent ozone oxidation rate $k_{net} = (6.2 \pm 1.1) \times 10^{-19}$ cm^3 molecule^{-1} s^{-1} (with ± 20% additional potential experimental error, *e.g.*, associate with instrumental accuracy) provides an approximate lifetime of gaseous mercury, shown in Table 2; about 2–8 days over a polluted city and 19–38 days in more remote areas. However, in presence of likely reduction mechanisms (aqueous or heterogeneous), this calculated lifetime should be significantly prolonged. Reduction mechanisms in aerosols, fogs and clouds, as well as on the interfaces are suggested and we believe that this calculation is merely reflect the importance of oxidation schemes due to ozone initiated reactions of elemental mercury. Our results indicate that in environmental conditions (such as in aerosols, cloud droplets, in ice flakes, *etc.*), the gas-phase ozone-initiated reaction of elemental mercury can be enhanced significantly. The observed gas-phase initiated oxidation rate loss of mercury can be affected by several environmental conditions. Reactions of mercury and ozone will be catalyzed in cloud,

aerosols and fog droplets and air–water–ice–soil interfaces. More detailed mechanistic studies however, particularly involving surfaces, are required.

Table 1 k_{net} Dependency on [H_2O] each point represents a minimum of 6 experiments; and k_{net} dependency on [CO]. Each point represents a minimum of 6 experiments

Relative humidity (± 2%)	$k_{net} \times 10^{19}$/cm^3 molecule^{-1} s^{-1} (95% error)	[CO]/pp thousand	$k_{net} \times 10^{19}$/cm^3 molecule^{-1} s^{-1} (95% error)
0	17.8(1.2)	0	17.8(1.2)
5	19.7(2.8)	0.8	19.3(1.7)
10	20.7(8.4)	1.6	24.7(7.7)
20	19.2(6.2)	3.2	41.2(6.8)
40	26.3(7.0)	4.8	50.3(8.0)
60	31.3(5.0)	6.4	59.7(8.5)
80	26.0(4.7)		
95	24.8(2.7)		
≥ 100	Non-linear		

Table 2 Mercury life time estimation upon oxidation initiated by ozone in various regions of the globe. The reduction reactions are not included, and they are expected to increase the listed values in this table significantly. Typical summertime daily maximum ozone concentrations used to estimate Hg^0 lifetimes for RH = 0% and T = 298 K (excluding Hg(II) reduction/re-emission)

Region	Ozone/ppb[a]	Hg^0(g) lifetime/days ($1/k_{net}[O_3]$; $k_{net} = (6.2 \pm 1.1) \times 10^{-19}$ cm^3 molecule^{-1} s^{-1})
Urban-suburban	40–120	6–19
Rural[35]	15–40	19–51
Marine boundary layer[36]	10–20	38–76

[a] 1 ppb = 2.46×10^{10} molecules cm^{-3} (T = 298 K, p = 1 atm).

Acknowledgements

We would like to thank Andrew Ryzhkov, Kirk Peterson, for helpful comments, Ed Hudson as a perpetual source of advice, Morteza Vahedpour for initiating the project, and a thanks to NSERC, CFI, and Environment Canada for continued financial support. We are grateful to two anonymous reviewers for their constructive comments.

References

1. O. Lindqvist and H. Rodhe, *Tellus B*, 1985, **37**, 136 .
2. R. P. Mason, F. M. M. Morel and W. F. Fitzgerald, *Geochim. Cosmochim. Acta*, 1994, **58**(15), 3191 .
3. T. Bergan, L. Gallardo and H. Rodhe, *Atmos. Environ.*, 1999, **33**, 1575 .
4. R. L. Shia, C. Seigneur, P. Pai, M. Ko and N. D. Sze, *J. Geophys. Res., [Atmos.]*, 1999, **104**, 23747 .
5. C. Seigneur, K. Vijayaraghavan, K. Lohman, P. Karamchandani and C. Scott, *Environ. Sci. Technol.*, 2004, **38**, 555 .
6. S. E. Lindberg and W. J. Stratton, *Environ. Sci. Technol.*, 1998, **32**, 49.
7. W. H. Schroeder, G. Yarwood and H. Niki, *Water, Air, Soil Pollut.*, 1991, **56**, 653 .
8. L. Poissant, M. Pilote, C. Beauvais, P. Constant and H. H. Zhang, *Atmos. Environ.*, 2005, **39**, 1275 .
9. P. A. Ariya, A. P. Dastoor, M. Amyot, W. H. Schroeder, L. Barrie, K. Anlauf, F. Raofie, A. Ryzhkov, D. Davignon, J. Lalonde and A. Steffen, *Tellus B*, 2004, **56**, 397 .
10. R. Ebinghaus, H. H. Kock, A. M. Coggins, T. G. Spain, S. G. Jennings and C. Temme, *Atmos. Environ.*, 2002, **36**, 5267 .
11. F. M. M. Morel, A. M. L. Kraepiel and M. Amyot, *Annu. Rev. Ecol. Syst.*, 1998, **29**, 543 .
12. B. Pal and P. A. Ariya, *Environ. Sci. Technol.*, 2004, **38**, 5555 .
13. B. Pal and P. A. Ariya, *Phys. Chem. Chem. Phys.*, 2004, **6**, 572 .
14. F. Raofie and P. A. Ariya, *Environ. Sci. Technol.*, 2004, **38**, 4319.
15. P. A. Ariya, A. Khalizov and A. Gidas, *J. Phys. Chem. A*, 2002, **106**, 7310 .
16. R. Menke and G. Wallis, *Am. Ind. Hyg. Assoc. J.*, 1980, **41**, 120 .
17. A. Iverfeldt and O. Lindqvist, *Atmos. Environ.*, 1986, **20**, 1567 .

18. J. G. Calvert and S. E. Lindberg, *Atmos. Environ.*, 2005, **39**, 3355 .
19. A. Sumner, C. Spicer, J. Satola, R. Mangaraj, K. Cowen, M. Landis, R. Stevens and T. Atkeson, Environmental Chamber Studies of Mercury Reactions in the Atmosphere, in *Dynamics of Mercury Pollution on Regional and Global Scales*, 2005, p. 193 .
20. B. Hall, *Water, Air, Soil Pollut.*, 1995, **80**, 301 .
21. S. Coquet and P. A. Ariya, *Int. J. Chem. Kinet.*, 2000, **32**, 478 .
22. D. Daumont, J. Brion, J. Charbonnier and J. Malicet, *J. Atmos. Chem.*, 1992, **15**, 145 .
23. L. M. Arin and P. Warneck, *J. Phys. Chem.*, 1972, **76**, 1514 .
24. D. H. Stedman and H. Niki, *Environ. Lett.*, 1973, **4**, 303.
25. R. Gutbrod, S. Meyer, M. M. Rahman and R. N. Schindler, *Int. J. Chem. Kinet.*, 1997, **29**, 717 .
26. O. Horie and G. K. Moortgat, *Chem. Phys. Lett.*, 1998, **288**, 464 .
27. F. Kramp and S. E. Paulson, *J. Phys. Chem. A*, 1998, **102**, 2685 .
28. J. Sommar, M. Hallquist, E. Ljungström and O. Lindqvist, *J. Atmos. Chem.*, 1997, **27**, 233 .
29. K. Aurivillius, *Acta Crystallogr.*, 1956, **9**, 685.
30. G. B. Taylor and G. A. Hulett, *J. Phys. Chem.*, 1913, **17**, 565 .
31. J. A. Tossell, *J. Phys. Chem. A*, 2006, **110**, 2571 .
32. B. C. Shepler and K. A. Peterson, *J. Phys. Chem. A*, 2003, **107**, 1783.
33. A. L. Sumner, E. J. Menke, Y. Dubowski, J. T. Newberg, R. M. Penner, J. C. Hemminger, L. M. Wingen, T. Brauers and B. J. Finlayson-Pitts, *Phys. Chem. Chem. Phys.*, 2004, **6**, 604 .
34. J. Munthe, *Atmos. Environ.*, 1992, **26**, 1461 .
35. J. F. Meagher, N. T. Lee, R. J. Valente and W. J. Parkhurst, *Atmos. Environ.*, 1987, **21**, 605
36. A. M. Thompson, J. E. Johnson, T. S. Bates, K. C. Kelly, A. L. Torres, E. Atlas, J. P. Greenberg, N. M. Donahue, S. A. Yvon and E. S. Saltzman, *J. Geophys. Res., [Atmos.]*, 1993, **98**(D9), 16955 , PBD: 20 Sep 1993.